Scattering loss estimation using 2D Fourier analysis and modelling of sidewall roughness on optical waveguides

**E. Jaberansary, T. B. Masaud, M. M. Miloevic, M. Nedeljkovic, G. Z. Mashanovich,
H. M. H Chong
Nano Research Group, Electronics and Computer science,
Faculty of Physical and Applied Sciences, University of Southampton, SO17 1BJ, UK**

Manuscript received March 17, 2012; revised November 19, 2013. First published December ..., 2013.

Abstract: We report an accurate scattering loss 3D modeling technique of sidewall roughness of optical SOI waveguides based on Fourier and Finite Difference Time Domain (FDTD) analysis methods. The Fourier analysis method is based on the image recovery technique used in magnetic resonant imaging. Losses for waveguides with isotropic and anisotropic roughness are calculated for wavelengths ranging from 1550 nm to 3800 nm and compared with reported results in literature. Our simulations show excellent agreement with published experimental results and provide an accurate prediction of roughness-induced loss of 3D arbitrary shaped optical waveguides.

Index Terms: Roughness, Scattering loss, Optical Waveguide

1. Inroduction

Advances in optical waveguide technology allow the integration of optical devices for high performance operations [1]. Semiconductor and dielectric optical waveguides are dominantly considered as the basic building block of complex optical integrated circuits. As the size shrinks down toward nanoscale, some physical waveguide parameters become significant and hence limit the range of operation [2]. The TM mode leakage loss is an example which can be particularly important for reduced dimensions and certain geometries [3]. One of the other major issues is the radiation loss caused by the scattering of light due to sidewall roughness of the waveguide. Sidewall roughness is a technological process dependent factor. The scattering loss of optical waveguide varies with waveguide geometry, mode polarization state, and roughness parameters. For example, the scattering is more considerable when the optical path is long and also for small and high index contrast waveguides [4]. The effect of scattering on propagation loss in silicon waveguides can be observed in the range from low absorption wavelength region in the near-IR (NIR) to the mid-IR (MIR) wavelength area [5].

The induced loss due to sidewall roughness can be considerably reduced by optimizing the fabrication process [6], [7]. Successful demonstrations show that silicon oxidation can be used to reduce the surface roughness and losses of strip waveguides [6]. This will however change the waveguide cross section dimensions which are not desirable in precisely designed structures. Atomic Layer Deposition (ALD) has been recently studied as an alternative [7]. The scattering loss is considered as an unavoidable feature of nanoscale waveguides and has to be taken into account in the design of photonic elements.

Optical waveguide roughness has been theoretically studied since 1969 when Marcuse established a complete but quite complex analytical expression applicable for 2D planar waveguides [8]. Payne and Lacey developed a simplified expression by excluding the unnecessary far field term [9]. This expression is hence less complex and includes waveguide physical parameters. It is also commonly accepted as an analytical description for 2D planar waveguides and widely referred in the literature for comparison with experimental results [4], [10], [11]. There were also attempts to extend Payne and Laceys model into 3D structures [12]. However many of these works have been managed to exnted different analytical theories for certain situations and applications (i.e. high or low contrast weaveguide and circular waveguides) [13], [14]

In this paper we report how scattering loss can be accurately estimated from randomly generated roughness on the sidewalls of 3D optical waveguides. The method to deduce roughness is developed based on an inspiration from the fundamentals of Magnetic Resonance Imaging (MRI) technique [15]. Depending on the fabrication process as well as anisotropic sidewall roughness, isotropic sidewall roughness is also expected [16]. For a better comparison the model is therefore designed to accurately implement both types of roughness, making this work distinct from other 3D waveguide studies where the sidewall roughness is only anisotropic. The model uses two main parameters, which characterize the roughness, the correlation length and the root mean square (RMS) roughness, which is given by a standard deviation from the averaged flat surface. A randomly generated k-space is virtually created in commercial software, Lumerical script environment, which can also be independently executed in any scripting environment. The k-space stores all phase and wavelength information of any surface. It is then filtered according to the real roughness data extracted from AFM (Atomic Force Microscopy) images, and the actual surface is realized by applying the Fourier Transform (FT) on the filtered k-space. The generated surface roughness is then implemented as sidewalls of the optical waveguide. With this technique, anisotropic and isotropic sidewall roughness features can be accurately modeled based on surface data extracted from AFM. We use 3D FDTD technique to estimate the induced loss due to the sidewall roughness of the optical waveguide structure. The accuracy of the loss model is also dependent on the mesh resolution in FDTD. Our final results are compared with other published work.

Our later result shows that the model has a comparable accuracy to the commonly used scattering loss estimation technique developed by Payne and Lacey [9]. The accuracy can be however improved by using a cluster with more available memory space in order to provide finer mesh settings. Unlike Payne and Laceys model that is originally developed for sidewalls of 2D structures, our model can be used for 3D structures with sidewalls that have anisotropic, isotropic and mixture of isotropic and anisotropic roughness. Our model can be also implemented on arbitrary waveguide shapes such as cylindrical and triangular geometries and high or low contrast waveguides, where Payne and Laceys model is not applicable. Roughness can be also deduced on top surface of the waveguide if it is required. In addition the model can be widely used in any commercial software using FDTD algorithm in order to estimate the effect of scattering loss for various photonic devices and applications.

2. Generation of random roughness on rectangular optical waveguide sidewalls

The method used to model roughness is based on Fourier analysis approach used in magnetic resonance imaging (MRI)technique [15], [17]. The roughness of a flat surface can be considered as a two dimensional image where each point (pixel) has different random correlated intensities. The correlation of these distributed random intensities in the image is defined by a suitable Auto Correlation Function (ACF). The ACF explains how random variables are related statistically. The ACF of a random roughness is characterised by correlation length, Lc, and mean square deviation, 2, from a flat surface without irregularities. The most commonly used ACFs for process dependant roughness are exponential and Gaussian [9]. AFM measurements of silicon optical waveguide surface roughness have demonstrated that Gaussian ACF is a realistic model for the statistics of surface roughness of a variety of waveguides [9]. The Gaussian ACF is expressed as:

$$R(u) = \sigma^2 exp(-\frac{u^2}{L_c^2}) \tag{1}$$

Here the image is treated as a random two-dimensional signal. The Fourier spectrum of this signal is generally represented in a different coordinate so called k-space. K-space is a 2D Fourier transform of the original image in real space as illustrated in Figure 2. Each point in k-space is a complex number where its frequency and phase values are obtained in horizontal and vertical axis respectively. Hence, it contains all required frequency, phase and amplitude information of the image in real space and typically has the same number of rows and columns as the original image. Low frequency components (long wavelengths) are stored around and at the middle and high frequencies components (short wavelengths) near the periphery region. Low spatial frequencies produce only waves with long wavelength characteristics in the original image. These waves only provide contrast information and give little data for the edges. On the other hand high spatial frequencies eliminate many contrast information in the resultant image, since contrast data is mainly formed by waves only with long wavelength characteristics.

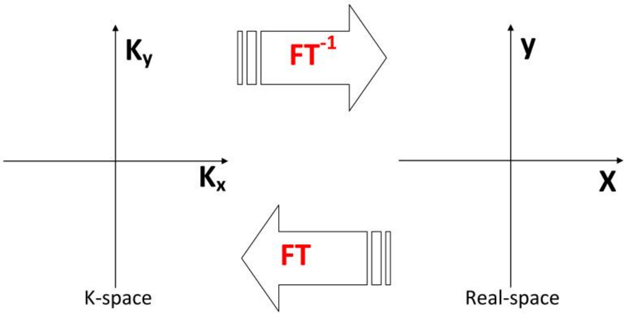

Fig. 1. The real and K-space relation according to Fourier analysis; in the K-space we express the magnitude, the wavelength and the phase of all signals that exist in the real image.

We preferably want to implement the roughness on the sidewalls of a rectangular waveguide. The roughness is initially generated on a flat surface S that is later mapped onto the sidewalls. In order to assign position to different points of the surface S, it has to be mapped in to the real space. At this stage the surface is considered to be completely flat without having roughness. This means the intensity of all points in the surface is initiated to be zero and hence we call it unoccupied real space. In order to expresses our proposed surface S as an unoccupied real space, the surface S is represented by an n by m matrix. The matrix represent surface S is named as S_c. The entries of the matrix S_c expresses the position of the associated element in the surface S while the values of the entries express the height level in the surface S. The roughness will be generated above the surface by assigning correlated intensities to the elements of th matrix S_c.

The discrete real space is virtually created by defining two position matrixes X and Y that has the same dimension as matrix S_c. This is shown in Figure 2. They respectively represent x and y components of the position vector of each element (point) in the matrix S_c (surface). Hence any element (intensity) in matrix S_c has an equivalent element in X and Y that specify its position in x and y coordinate of the real space.

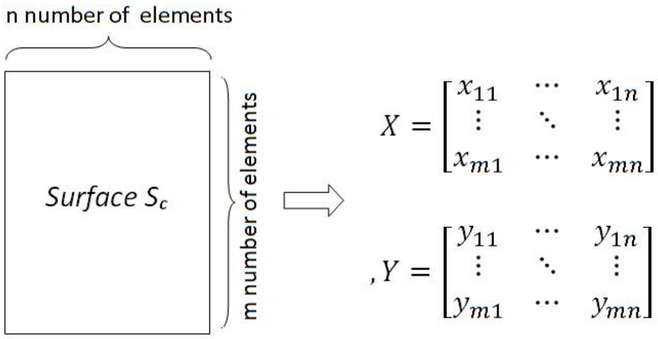

Fig. 2. The creation of discrete real space that contains n×m elements. X and Y respectively store the x and y coordinates of all elements in the surface S_c.

In this case:

$$\begin{aligned} x_{11} = x_{21} = \ldots = x_{m1} \\ \vdots \\ x_{1n} = x_{2n} = \ldots = x_{mn} \end{aligned} \tag{2}$$

since X only represent the x components of the position vector. For the same reason,

$$\begin{aligned} y_{11} = y_{12} = \ldots = y_{1n} \\ \vdots \\ y_{m1} = y_{m2} = \ldots = y_{mn} \end{aligned} \tag{3}$$

Once the real space is created the relevant k-space can be also formed. Considering Equations 4 and 5 , the required spatial wavevectors $\mathbf{K}_x$ and $\mathbf{K}_y$ of an unfilled k-space associated with a Fourier transform of a function of the elements of X and Y is generated. The corresponding k-space is shown in Figure 3a.

$$K_x = \frac{2\pi}{dx.n} x_{nm} \tag{4}$$

$$K_y = \frac{2\pi}{dx.n} y_{nm} \tag{5}$$

Here *dx* represents the spacing between the values of the input *x*, *n* and *m* denote the length of x and y respectively. In addition, both *x* and *y* domain is extended from negative to positive values and therefore the generated k-space includes both negative and positive frequencies and phases. When the k-space is constructed, it is filled by uniform random numbers Figure(3b. Each point in k-space has now a random value, which expresses the amplitude of a trigonometric signal at specific frequency and phase. These randomly generated data are stored in a new *n* by *m* matrix that is called **Z**. The matrix **Z** is used to express the k-space of the matrix S_c. According to Fourier theory the superposition of all of the signals stored in **Z** will form the final surface S_c. This is where the ACF is used. Applying ACF to the matrix **Z** provides a low pass filter that removes high frequency components in the k-space, such that the resultant image does not have much of the edge information. This removes the edge details of previously generated uncorrelated random heights. The filtered data is then stored in a matrix called $\mathbf{Z}_{filtered}$. The resultant K-space, is shown in Figure 3c. According to Equation 1 the Gaussian ACF is related to the correlation length L_c, and mean square deviation σ^2. Here sigma σ is defined as:

$$\sigma = Z(n,m) - \frac{\sum_0^n \sum_0^m Z(n,m)}{n \times m} \tag{6}$$

A certain point at *r* position in k-space $\sqrt{{K_x}^2 + {K_y}^2}$can be correlated with a point at $r + \sigma$ using Equation 7:

$$Z_{filtered} = Z(n,m)^2 \times exp - (\sqrt{{K_x}^2 + {K_y}^2}/L_c)\sigma = Z(n,m) - \frac{\sum_0^n \sum_0^m Z(n,m)}{n \times m} \tag{7}$$

The resulting values in k-space that are shown in Figure 3c are then transformed back to real space, as can be seen in Figure 3d;

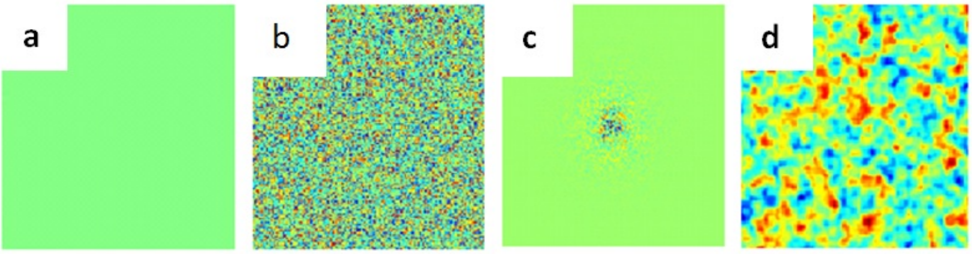

Fig. 3. The generation steps of roughness: a) Unoccupied k-space, a coordinate showing all available phase and wavelengths for the signals in real image b) k-space with randomly generated elements, to include magnitude of each signal c) Filtered k-space to remove the edge information d) the resulting roughness in real space.

Figure 3d shows the roughness in real space is completely random and characterised to retain the isotropic behaviour. Two different randomly generated S_c surfaces can be imported on both sidewalls of 3D planar waveguide for further studies on propagation loss characteristics of optical waveguides. Isotropic sidewall roughness and loss analysis has been previously reported in [16]. Accurate AFM/SEM images show even on sidewalls with anisotropic roughness, there is still a degree of isotropic roughness features. The difference is illustrated in Figure 4. Such a characteristic is often ignored in scattering loss evaluations and mathematically reported roughness models.

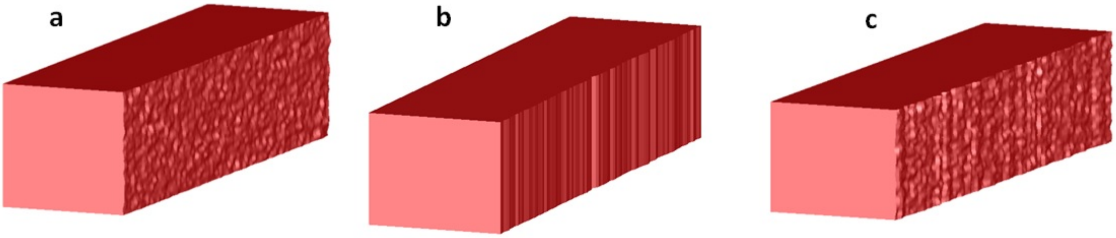

Fig. 4. Different type of roughnesses, a) Isotropic b) anisotropic, c) mixture of isotropic and anisotropic roughness

Isotropic roughness is simply achievable, once the roughness surface in real space is created. In order to generate anisotropic roughness the following steps is performed. A one dimensional random roughness profile is configured by accessing a random row of the matrix that expresses surface S_c. When such a profile is repeated in y direction, a new matrix with identical row will be formed. This newly constructed matrix, $S_{anisotropic}$ is used to represent the completely anisotropic surface.

The integration of S_c and $S_{anisotropic}$ anisotropic will form the optimal sidewall roughness model that is anisotropic in y direction, but still has a level of isotropic behaviour. This procedure is graphically explained in Equation 8.

$$\begin{matrix} x_{11} \cdots x_{1n} \\ \vdots \ldots \vdots \\ x_{m1} \cdots x_{mn} \end{matrix} + \begin{matrix} x_{11} \cdots x_{1n} \\ \vdots \ldots \vdots \\ x_{11} \cdots x_{1n} \end{matrix} = \begin{matrix} x_{11} + x_{11} \cdots x_{1n} + x_{1n} \\ \vdots \ldots \vdots \\ x_{m1} + x_{11} \cdots x_{mn} + x_{1n} \end{matrix} \tag{8}$$

The mixture is formed by superimposing a random $S_{anisotropic}$ matrix to a random S_c. The matrixes $S_{anisotropic}$ and S_c can have either different or identical roughness properties if it is required. All three types of roughnesses from Figure 4 are fully attainable using the same modelling technique. This makes our model reliable and applicable for roughness studies in arbitrary waveguide devices. In addition the isotropic roughness can be applied on top surface of the waveguide if required.

3. Fabrication and measurements

Ion bombardment in the dry etch process is considered to be one of the major origins of sidewall roughness. This kind of roughness can be significantly reduced using a low gas pressure and a low radio-frequency power [18], [19]. Pattern transfer during the etch prcocess is also considered as one of the origins of sidewall roughness [19]. We fabricated silicon waveguide structres using 500 nm thick SOI and 2 μm thick BOX layer to realise 500 nm width waveguide. The other sample contains a 220 nm width waveguide on top of the 3 μm BOX layer.

Atomic Force microscopic system with special high aspect ratio probe is used to generate multiple AFM images of the optical waveguide. The tip length of the probe is 2 μm and tip radius 10 nm. Figure 5b shows a sample 3D view of the AFM image of the silicon optical waveguide we have fabricated together with its SEM image. The two main roughness parameters, RMS and correlation length is extracted from the edge of sidewalls in AFM image. The RMS is extracted directly from the profile and the correlation length is found from the Autocorrelation function of the profile and equals to the minimum length that makes the normalized autocorrelation minumim ($\approx$ zero). The SEM image of the fabricated waveguide is also shown in Figure 5a The reproducible RMS of 5 nm and L_c of 45 nm were obtained from multiple samples.

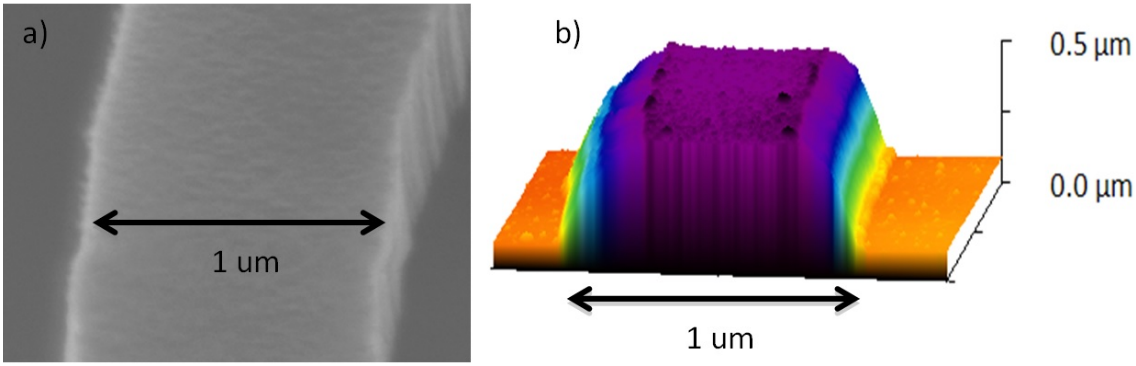

Fig. 5. a) SEM image of the fabricated waveguide, b) 3D AFM view of the fabricated waveguide. The waveguide has 500 nm height and 1000 nm width. The roughness parameters are extracted from the sidewall of this waveguide.

The dimensions of the waveguides we fabricated are 1000 nm by 500 nm as shwon in Figure 5. At this dimension, the waveguide can be single mode in the MIR. Once the roughness parameters are extracted from the sidewall of the waveguide they can be implemented into the simulation model to estimate the scattering loss.

4. Simulations and Discussion

The sidewall roughness parameters of the waveguide are extracted from its AFM measurements and imported to the roughness model in order to demonstrate the capability of this technique to estimate total scattering loss. In addition to fabricated waveguide explained above, various waveguides with obtainable roughness features can be also used for the same purpose as will be explained later.

The roughness model has been successfully configured in FDTD Lumerical software package and MATLAB environment. However, in order to run scattering loss simulations of the waveguides, it is preferred to use FDTD Lumerical package, because of its particular functionality and supportive features.

The fundamental TE mode is launched into the Si waveguide at a certain wavelength (i.e 1550 nm and 3800 nm) Two power monitors record the power transmission data through the waveguide. The first monitor is adjusted at the entry point of the optical waveguide to collect all transmission power information before the light is scattered with generated sidewall roughness. The second one stores these data after 100 μm length. Hence the scattering loss can be obtained in dB per unit of length.

The calculation of loss using such a method becomes complicated since the problem is numerically very large. A very fine mesh setting is necessary in order to resolve the features on the 3D waveguide sidewalls. This substantially increases the computational time. In addition the time-step must be reduced in order to keep within the Courant limit which makes the calculation time even longer [20]. Although this problem seems to be the major issue to achieve accurate results, tradeoffs in mesh settings can be applied to obtain reasonably accurate results.

We demonstrate the scattering loss by simulating the propagation of light in optical waveguides with the isotropic and anisotropic roughness. Our simulation results are compared with other mathematical models and a number of published results. However, the comparison with reported results in literature is difficult since there are various physical parameters that affect the losses. These parameters are mainly related to the cross section of the optical waveguide, the wavelength of light for given dimensions and also the statistical properties of the sidewall roughness.

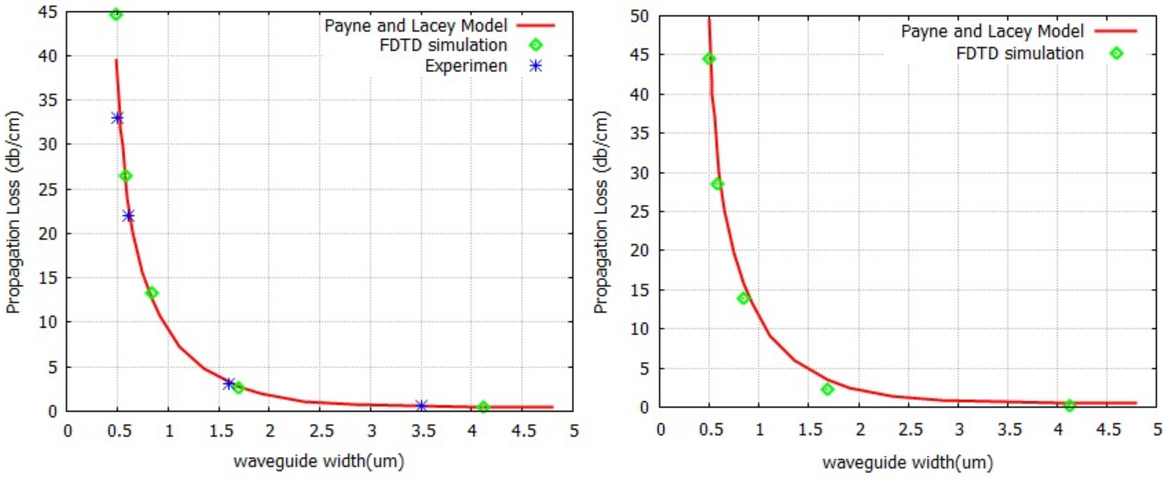

Fig. 6. Comparison of scattering loss of Si waveguides with different widths obtained from reference [21], Payne and Lacey, and our model for a)A SOI waveguide with a 1 μm deposited layer ofSiO_2 added on top of the 0.2 μ. b) SOI waveguide with no additional SiO_2 layer on top.in both cases Here Lc is 50 nm and σ is 9 nm.

We initially investigate the effect of the reduction in waveguide dimensions on the transmission loss. We calculated the transmission loss in three optical waveguides with different sidewall roughness styles. The SOI waveguides have a 200 nm fixed height and width varying from 400 nm to 4.5 μm.These dimensions provides high aspect ratio guide that can help to compare results with estimations obtained by Payne and Laceys 2D model [9]. The roughness parameters that are used are L_c=50nm and σ=9 nm. These are the values measured from identical waveguides in [21].

We consider the waveguide in two different situations. Firstly a deposited 1 μm layer of SiO_2 is added on top of the 0.2 μm SOI waveguide for an accurate comparison to the experimental results obtained in [21].In the other case the additional SiO_2 layer is not applied. The effect of size reduction on propagation loss is shown for both cases in Figure 6a and b respectively. Here waveguides have anisotropic rough sidewalls with a level of isotropic behavior. The isotropic statistical components are considered to be 5 times larger than anisotropic statistical component. Having fully anisotropic sidewall roughness gives identical values to those shown in Figure 6a and b. However Our other results show that the propagating mode in optical waveguide with completely isotropic sidewall roughness has higher scattering. The loss is as low as 2 dB/cm for waveguide width above 2.5 μm, indicating low scattering losses at the core - cladding interface. However, losses rapidly increase for widths below 2.5 μm and are as high as 44 dB/cm for 300 nm wide waveguides due to increased interaction between the mode propagating in the waveguide and the sidewalls. Clearly form the Figure 6 a, this is again in excellent agreement with the results reported in [21].

We also use the analytical approach by Payne and Lacey and the following expression to obtain scattering loss [9].

$$\alpha = 4.34\frac{\sigma^2}{\sqrt{2}K_0 d^4 n_1} g.f \tag{9}$$

Here α is the waveguide scattering loss in dB per unit length, σ is the RMS deviation, k_0 is the free space wave vector, d and n_1 are the waveguide half width and refractive index of Si core, respectively. Function g is determined purely by the waveguide geometry and f is a function of correlation length and other various parameters defined by Payne and Lacey [9]. In general the RMS and correlation length of the sidewall roughness can be extracted from the AFM images. The calculated scattering loss based on this approach is also shown in Figure 6 a and b. As can be seen the trend of our simulation results is in an excellent agreement with experimental measurements obtained by Lee et al. [21] and theatrically estimated by Payne and Lacey. The validity of this trend is completely retained for uncovered SOI waveguide in figure 6 b and still stays in a good agreement with Payne and Lacey calculated results. This result shows that when we have fixed roughness data (RMS and correlation length) and varying geometrical parameter (width or height), comparable estimations can be obtained using either Payne and lacy [9] or our approach.

Work	Dimension nm×nm (W×H)	Correlation Length(nm)	RMS(nm)	Loss (dB/cm) measured	Loss(dB/cm)- Our Simulations		
					Isotropic	Anisotropic	Mixed isotropic and anisotropic
Our First model (at 1500nm)	330×220	45±5	5±1	33	36.43	29.84	28.65
Our second model (at 3800nm)	1000×500	45±5	5±1	10.2	11.06	10.04	10.53
(1550nm)	445×650	225	5	2.1±0.6	2.6	1.72	1.79
[16](1550nm)	445×220	50	2	3.6±1	5.2	4.5	4.2
[21](1550nm)	500×200	50	9	33	47.32	36.3	36.1
[11](1550nm)	800×1800	225	5	1.1±1	3.30	2.71	2.34
[11](1550nm)	1000×1800	180	9	2.25±0.1	4.2	3.65	3.32
[11](1550nm)	1000×1800	160	13.5	6.5±1.5	9.63	8.94	8.16

TABLE I

COMPARISON OF THE RESULTS OBTAINED FROM OUR MODEL WITH A NUMBER OF EXPERIMENTAL OR CALCULATED MODELS. THE FIRST ROW CORRESPONDS TO THE WAVEGUIDE THAT IS SHOWN IN FIGURE 6 WHERE THE DATA IS DIRECTLY EXTRACTED FROM THE AFM IMAGE AND IMPORTED INTO THE LUMERICAL. THE SECOND ROW IS THE RESULT FOR A WAVEGUIDE WITH ARBITRARY DIMENSIONS. THE OTHER RESULTS THAT ARE SHOWN HERE, PROVE THE VALIDITY OF OUR MODEL AS IT MATCHES OTHER REPORTED EXPERIMENTAL WORK.

From Figure 6, the interaction of the mode with the sidewalls is strongly enhanced when the waveguide cross-section is decreased. Therefore an accurate comparison can only be possible for optical waveguides with comparable cross-sections (comparable propagation constants) and geometry. We use two waveguide samples with two different cross section sizes. The first sample is chosen to be 220 nm by 330 nm in height and width respectively while the second one has 1000 nm width and 500 nm height. These dimensions make the cross section of the optical waveguide moreidentical to other reported works in the literature that we are referring to. The wavelength is again fixed at 1550 nm. In table I our scattering loss simulation results, using the three roughness models, are compared to several published experimental results.

In the second work we simulate a large waveguide shown in Figure 5 in MIR wavelength range at 3.8 μm where the waveguides operates in single mode. . All other dimensions are ranged between 300 nm to 650 nm in height and 300 nm to 1000 nm in width. The statistical parameters (RMS and L_c) are process dependent factors and therefore they vary in a wider range. From table I it can be seen that the simulation results stay in a very good agreement with experimental reported data. It is also important to remember that the loss is measured applying different measurement techniques such as Fabry-Perot or the cut-back.

Our AFM measurements shows that the anisotropic behaviour of the sidewall roughness is more enhanced compared to its isotropic characteristics. However in all our samples the rms we measured for anisotropic roughness is at least 7 times larger than measured rms for isotropic roughness of a single rough sidewall surface. This makes anisotropic behaviour the dominant component in the mixed case as can be seen in Table I. Furthermore, form the data it seems that anisotropic roughnesses and the mixed isotropic and anisotropic roughnesses more realistically represents the form of actual sidewall roughness, as confirmed by direct measurement of the sidewall roughness.

Based on the data comparison in Table I and the discussion on the relationship between the waveguide dimension and the loss, we can extend our model to show the dependence of loss on sidewall roughness parameters for given waveguides. Figure 7 graphically illustrates the scattering loss dependence on the variation of correlation length when when σ is 5 nm. . Here we used a SOI waveguide that is 220 nm by 330 nm in height and width respectively. This waveguide has relatively low aspect ratio.

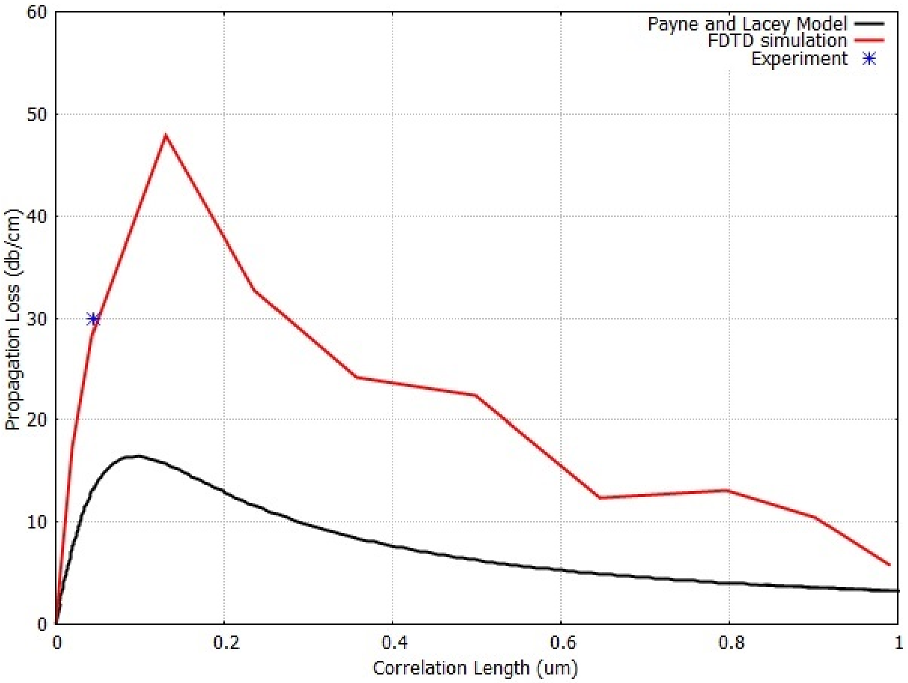

Fig. 7. Propagation loss against the correlation length of the sidewall roughness Our estimated results is compared with Payn and Lacey's model [10] and our experimental result.

Figure 7 shows that our FDTD simulations in comparision with the predicted results obtained by Payne and Lacey's model [9]. The simulation results show the validity of our experimental data. However for this relatively low aspect ratio waveguide the Payne and Lacy estimations does not appropriately match to our FDTD simulations. As expected from the theory [9], when the correlation length of the sidewall roughness is longer than the effective wavelength the scattering loss is reduced. This is because the variation along the direction of propagation is much larger than the effective wavelength. However, having a very short correlation length causes the waveguide boundary to change very fast. Therefore the propagating mode cannot determine the details of the sidewall and consequently the scattering loss is reduced again. The interaction between the propagating mode and sidewall roughness is maximized when the correlation length is not very short and very long compared to the effective wavelength.

5. Conclusion

We have successfully demonstrated 3 types of 3D sidewall roughness models that are used to analytically estimate the propagation loss in Si photonic waveguides. The simulation results are in excellent agreements with previously published data and Payne and Lacey's analytical method. The main roughness parameters, correlation length and rms or standard deviation are extracted from multiple AFM images of several samples. Using the model, the final scattering loss is calculated and compared for wires with isotropic and anisotropic sidewall roughness. The good agreement between the results proves the applicability of our model for accurate prediction of roughness-induced loss using only three main parameters. We have also shown how our numerical method is valid in different situations such as high and low aspect ratio structures where other analytical model may decline.It is also possible to implement this model into arbitrary waveguide shapes such as cylindrical and triangular geometries. andadditional surface roughness can be also deduced on top surface of the waveguide if it is required.

References

[1] Ed. G. T. Reed, *Silicon photonics - the state of the art.* Wiley-Interscience, 2008.

[2] J. P. R. Lacey and F. P. Payne, "Radiation loss from planar waveguides with random wall imperfections," *Optoelectronics (see also IEEE Proceedings-Optoelectronics), IEEE Proceedings J*, vol. 137, no. 4, p. 282288, 1990.

[3] M.A. Webster, R. Pafchek, A. Mitchell, and T. Koch, "Width dependence of inherent tm-mode lateral leakage loss in silicon-on-insulator ridge waveguides," *Photonics Technology Letters, IEEE*, vol. 19, no. 6, pp. 429–431, 2007.

[4] C. G. Poulton, C. Koos, M.f. Fujii, A. Pfrang, T. Schimmel, J. Leuthold, and W. Freude, "Radiation modes and roughness loss in high index-contrast waveguides," *IEEE Journal of slelected topics in quantum electronics*, vol. 12, no. 6, pp. 1306–1321, 2006.

[5] G. Z. Mashanovich, M. M. Miloevic, M. Nedeljkovic, N. Owens, B. Xiong, E. J. Teo, and Y. Hu, "Low loss silicon waveguides for the mid-infrared," *Opt. Express*, vol. 19, no. 8, p. 71127119, Apr. 2011.

[6] D. K. Sparacin, S. J. Spector, and L. C. Kimerling, "Silicon waveguide sidewall smoothing by wet chemical oxidation," *Lightwave Technology, Journal of*, vol. 23, no. 8, p. 24552461, 2005.

[7] T. Alasaarela, D. Korn, L. Alloatti, A. Syntjoki, A. Tervonen, R. Palmer, J. Leuthold, W. Freude, and S. Honkanen, "Reduced propagation loss in silicon strip and slot waveguides coated by atomic layer deposition," *Opt. Express*, vol. 19, no. 12, p. 1152911538, Jun. 2011.

[8] M. Marcuse, "Mode conversion caused by surface imperfections of a dielectric slab waveguide," *Bell Syst. Technology Journal*, pp. 3187–3215, 1969.

[9] F. P. Payne and J. P. R. Lacey, "A theoretical analysis of scattering loss from planar optical waveguides," *Optical and Quantum Electronics*, vol. 26, no. 10, p. 977986, Oct. 1994.

[10] K. K. Lee, D. R. Lim, H. C. Luan, A. Agarwal, J. Foresi, and L. C. Kimerling, "Effect of size and roughness on light transmission in a Si/SiO2 waveguide: Experiments and model," *Applied Physics Letters*, vol. 77, no. 11, p. 16171619, 2000.

[11] K. P. Yap, A. Delge, J. Lapointez, B. Lamontagne, J. H. Schmid, P. Waldron, B. A. Syrett, and S.Jan, "Correlation of scattering loss, sidewall roughness and waveguide width in silicon-on-insulator (SOI) ridge waveguides," *Journal of Lightwave Technology*, vol. 27, no. 18, pp. 3999–4008, 2009.

[12] T. Barwicz and H. A. Haus, "Three-dimensional analysis of scattering losses due to sidewall roughness in microphotonic waveguides," *Lightwave Technology, Journal of*, vol. 23, no. 9, p. 27192732, 2005.

[13] M. Kuznetsov and H. Haus, "Radiation loss in dielectric waveguide structures by the volume current method," *Quantum Electronics, IEEE Journal of*, vol. 19, no. 10, p. 15051514, 1983.

[14] S.G. Johnson, M.L. Povinelli, M. Solvia Ci, A. Karalis, S. Jacobs, and J.D. Joannopoulos, "Roughness losses and volume-current methods in photonic-crystal waveguides," *Applied Physics B Lasers and Optics*, vol. 81, pp. 283–293, 2005.

[15] C. Westbrook, C. Kaut Roth, and J. Talbot, *MRI in Practice*. John Wiley & Sons, 2011.

[16] Y. Vlasov and S. McNab, "Losses in single-mode silicon-on-insulator strip waveguides and bends," *Opt. Express*, vol. 12, no. 8, p. 16221631, Apr. 2004.

[17] W P Dong and K J Stout, "Two-dimensional fast fourier transform and power spectrum for surface roughness in three dimensions," *Journal of Engineering Manufacture*, vol. 209, pp. 381–391, 1995.

[18] E. Z. Liangn, C. J. Huang, and C. F. Li, "Use of SiO2 nanoparticles as etch mask to generate si nanorods by reactive ion etch," *Journal of Vacuum Science Technology*, vol. 24, pp. 599–603, 2006.

[19] P. Dumon, W. Bogaerts, V. Wiaux, J. Wouters, S. Beckx, J. Van Campenhout, D. Taillaert, B. Luyssaert, P. Bienstman, D. Van Thourhout, and R. Baets, "Low-loss SOI photonic wires and ring resonators fabricated with deep UV lithography," *Photonics Technology Letters, IEEE*, vol. 16, no. 5, p. 13281330, May 2004.

[20] Karl S. Kunz and Raymond J. Luebbers, *The Finite Difference Time Domain Method for Electromagnetics*. CRC Press, 1993.

[21] K. K. Lee, D. R. Lim, L. C. Kimerling, J. Shin, and F. Cerrina, "Fabrication of ultralow-loss Si/SiO waveguides by roughness reduction," *Optics Letters*, vol. 26, no. 23, p. 18881890, 2001.